TPPP acts downstream of RhoA–ROCK–LIMK2 to regulate astral microtubule organization and spindle orientation

Yi-Wen Heng[1], Hong-Hwa Lim[2], Theresia Mina[1], Prayudi Utomo[1], Shaoping Zhong[3], Chwee-Teck Lim[3,4] and Cheng-Gee Koh[1,4,*]

[1]Division of Molecular Genetics and Cell Biology, School of Biological Sciences, College of Science, Nanyang Technological University, 60 Nanyang Drive, 637551, Singapore
[2]Institute of Molecular and Cell Biology, ASTAR, 61 Biopolis Drive, 138673, Singapore
[3]Division of Bioengineering and Department of Mechanical Engineering, National University of Singapore, 21 Lower Kent Ridge Road, 119077, Singapore
[4]Mechanobiology Institute, National University of Singapore, T-Lab, #05-01, 5A Engineering Drive 1, 117411, Singapore
*Author for correspondence (cgkoh@ntu.edu.sg)

Accepted 8 November 2011
Journal of Cell Science 125, 1579–1590

doi: 10.1242/jcs.096818

Summary

The actin cytoskeleton in eukaryotic cells undergoes drastic rearrangement during mitosis. The changes to the actin cytoskeleton are most obvious in the adherent cells, where the actin stress fibres are disassembled, and the cortical actin network becomes more prominent with concomitant increase in cell rigidity as cells round up and enter mitosis. Although the regulatory connections between the actin cytoskeleton and the early mitotic events are apparent, the mechanisms that govern these links are not well understood. Here, we report that LIMK1 and LIMK2, the downstream effectors of RhoA and ROCK, regulate centrosome integrity and astral microtubule organization, respectively. Surprisingly, LIMK1 and cofilin are not involved downstream of RhoA and ROCK in the regulation of astral microtubule organization. Instead, we find that LIMK2 acts through TPPP in the regulation of astral microtubule organization, whereas both LIMK1 and LIMK2 affect centrosome focusing. Both phenotypes are tightly coupled to spindle orientation in the mitotic cells. Thus, our results reveal a new regulatory link between the actin cytoskeleton and the mitotic spindle during the early stages of mitosis.

Key words: Actin cytoskeleton, Astral microtubule, Cortical rigidity, LIM kinases, Spindle orientation, Rho GTPases

Introduction

The actin cytoskeleton is a dynamic network that gives eukaryotic cells their characteristic shape. However, it undergoes extensive reorganization and remodeling during mitosis. Adherent cells, which adopt 'spread out' morphologies during interphase, exhibit a dramatic loss of stress fibres upon entering mitosis and become rounded. The cortical actin network becomes more prominent during this time, resulting in an increase in cortical rigidity. Upon completion of cell division, the daughter cells re-establish attachment to the extracellular matrix and, once again, attain the spread-out morphology. Treatment with actin-disruptive drugs, such as cytochalasin D and latrunculin B, results in delayed mitosis in both mammalian cells and fission yeast, suggesting that the cytoskeleton is important for efficient progression through the cell cycle (Gachet et al., 2001; Lee and Song, 2007). The correlation between cell shape changes and cell cycle progression clearly underscores a tight coupling of regulatory controls of the actin cytoskeleton and the cell division process (Heng and Koh, 2010).

The dynamics of the actin cytoskeleton are regulated by the Rho GTPases (Etienne-Manneville and Hall, 2002; Koh, 2006). CDC42, Rac1 and RhoA are the most studied among the Rho GTPases that have been identified thus far. CDC42 and Rac1 induce filopodia and lamellipodia, respectively, through WASP and WAVE signaling (Takenawa and Miki, 2001). RhoA, however, acts through ROCK and mDia1 (also known as DIAP1) to maintain cell contractility, actin stress fibres and focal adhesions (Burridge and Wennerberg, 2004). Downstream of ROCK are the LIM kinases, which are phosphorylated and activated by ROCK (Maekawa et al., 1999; Ohashi et al., 2000). The Rho GTPases are also involved in the regulation of cell cycle progression. Inhibition of the Rho GTPases using C3 toxin results in cell cycle arrest at G1 (Olson et al., 1995; Yamamoto et al., 1993). Similarly, the activity of RhoA has been implicated in the formation of the contractile acto-myosin ring at the cleavage furrow during cytokinesis (Bement et al., 2005).

The cortical actin and myosin at the cell cortex have important roles in the segregation of centrosomes and spindle assembly in mitotic cells (Kunda and Baum, 2009). This is evident by the observation that treatment with ROCK inhibitor (Y26732) or blebbistatin to inhibit the activity of non-muscle myosin II leads to the disruption of spindle assembly (Rosenblatt et al., 2004). Although RhoA, ROCK and myosin activities are partially required for cell rounding during mitosis, moesin contributes substantially to the cortical rigidity required for cell rounding and spindle stability (Carreno et al., 2008; Kunda et al., 2008). Consistent with the close connection between the actin cytoskeleton and cell cycle regulation, an RNAi screen for proteins that prevent multi-polar centrosomes in *Drosophila* S2

cells has identified many proteins involved in the control of the actin cytoskeleton (Kwon et al., 2008). However, despite these clear links, the signaling pathways and their effectors that functionally integrate actin cytoskeleton and mitotic progression are not fully elucidated.

In this study, we investigate specifically the consequences of perturbing the actin network at the onset of mitosis by using C3 transferase to inhibit the Rho GTPases and the ROCK inhibitor. We find that perturbing the actin network at the onset of mitosis leads to changes in the cortical rigidity and an increase in astral microtubule numbers. Consequently, spindle positioning and orientation are adversely affected. We have delineated the signaling pathway downstream of RhoA and ROCK, which regulates astral microtubule organization at early stages of mitosis. Surprisingly, whereas LIMK1 and cofilin are not involved, LIMK2 and TPPP are found to be important. Inhibition of Rho GTPases and ROCK also leads to defocusing of the centrosomes and involves both LIMK1 and LIMK2 as the key regulators. Thus, our results identify LIMK1 and LIMK2 as important effectors that act through different substrates to provide functional links between the actin cytoskeleton and spindle dynamics.

Results

Perturbation of actin cytoskeleton affects astral microtubule arrangement, centrosome integrity and spindle orientation

To understand how the progression through mitosis is affected by changes in actin cytoskeleton dynamics, we perturbed the actin cytoskeleton by using specific inhibitors of the Rho GTPase pathway and monitored the cellular changes as cells entered mitosis. Y27632, which inhibits ROCK1 and ROCK2, and C3 transferase, which inhibits RhoA, RhoB and RhoC were chosen for this study (Narumiya et al., 1990; Uehata et al., 1997). HeLa cells were treated with Y27632 and C3 transferase for 3 hours. The cells were then fixed and immunostained using anti-α-tubulin and DAPI, respectively. Metaphase cells (determined by staining with DAPI) were selected for analysis. Perturbation of the actin cytoskeleton was found to result in a less-defined mitotic spindle with a dramatic increase in the number of astral microtubules radiating from the spindle pole towards the cell cortex (Fig. 1A). The quantification of astral microtubules (Fig. 1B) showed that astral microtubule fluorescence was increased by 1.58 and 1.82 times with respect to the mitotic spindle when the cells were treated with Y27632 and C3 transferase, respectively.

These cells also showed a dramatic defocusing of the centrosomes when visualized using pericentrin staining (Fig. 1C), suggesting that the disruption of the actin network affects centrosome integrity. More interestingly, the inhibition of Rho GTPases or ROCK leads to spindle mis-orientation (Fig. 1D), possibly arising from the aberrant astral microtubule organization and centrosomes. Non-polarized adherent cells normally position their mitotic spindles almost parallel to the substratum (Thery et al., 2005; Toyoshima and Nishida, 2007). However, in cells treated with Y27632 or C3 transferase, the tilt-angle of the spindle was increased substantially. We then proceeded to identify the downstream effectors in the RhoA and ROCK pathway that regulate astral microtubule dynamics directly and/or centrosome focusing, thereby affecting spindle orientation.

Cortical rigidity and astral microtubule control

The cortical rigidity of the mitotic cells after treatment with C3 transferase and Y27632 was measured using a micropipette aspiration assay. As expected, disruption of the actin cytoskeleton by inhibition of RhoA and ROCK led to reduced cortical rigidity (Fig. 2A). Because the LIMKs are known substrates of ROCK, we examined the effect of LIMK-mutant constructs on cortical rigidity in Y27632- and C3 transferase-treated mitotic cells. The micropipette aspiration assay revealed that only the kinase-active LIMK2 (T484E) construct, but not its kinase-inactive mutant [LIMK2 (D430A)] or LIMK1 active (T508E) and inactive (D460A) mutants, was able to restore the reduction in cortical rigidity caused by Y27632 (Fig. 2B). However, none of the LIMK1 or LIMK2 constructs was able to rescue the diminished cortical rigidity in C3 transferase-treated cells. One possible reason is that the inhibition of RhoA but not ROCK affected the phosphorylation status of the ezrin, radixin, moesin (ERM) proteins (Fig. 2C). It has been reported that the phosphorylation status of moesin regulates the mitotic cortical rigidity in *Drosophila* S2 cells (Carreno et al., 2008; Kunda et al., 2008). Indeed, from our western analysis, we see an increase in phosphorylated ERM in mitotic cells (Fig. 2D). This observation is similar to that reported by Carreno and colleagues (Carreno et al., 2008), where they compared interphase S2 cells and pro-metaphase cells. Moreover, we also observe increased phosphorylated ERM levels upon overexpression of the wild-type or dominant-active RhoA (Fig. 2E). Neither active ROCK nor mDia affected the phosphorylation of the ERM proteins. Silencing both LIMK1 and LIMK2 also did not alter phosphorylated ERM levels (Fig. 2F). Taken together, these results suggest that perturbation of cortical rigidity leads to increased astral microtubule numbers, and that the RhoA–ROCK–LIMK2 pathway cooperates with the RhoA–moesin pathway to regulate the cortical rigidity.

LIMK2, but not LIMK1, regulates astral microtubules downstream of ROCK

Investigating the connections between the LIMK proteins and astral microtubules, we found that only the active LIMK2, but not LIMK1, was able to reverse the increased astral microtubule phenotype (Fig. 3A,B). This suggests that LIMK2 acts downstream of RhoA and ROCK to regulate the astral microtubule at metaphase of the cell cycle.

LIMK1 and LIMK2 are reported to localize differently at different stages of the cell cycle – LIMK1 is localized to the centrosomes whereas LIMK2 is localized to the mitotic spindles (Sumi et al., 2006). It is, therefore, possible that the different effects elicited by LIMK1 and LIMK2 are due to differences in their cellular locations. Immuno-staining with anti-LIMK2 antibodies confirmed that LIMK2 is indeed localized to the mitotic spindle in HeLa cells. However, this localization was lost when the cells were treated with C3 transferase and Y27632 (Fig. 3C). The proportion of cells showing LIMK2 spindle localization was reduced to ~40% when the Rho–ROCK pathway was inhibited (Fig. 3D).

The LIMK proteins phosphorylate cofilin at serine 3 and result in the inhibition of cofilin activity (Arber et al., 1998; Sumi et al., 1999; Yang et al., 1998). If cofilin is located downstream of LIMK2 in the regulation of astral microtubule organization, then active cofilin (S3A) would be expected to induce the astral microtubule phenotype. Although the wild type and active (S3A)

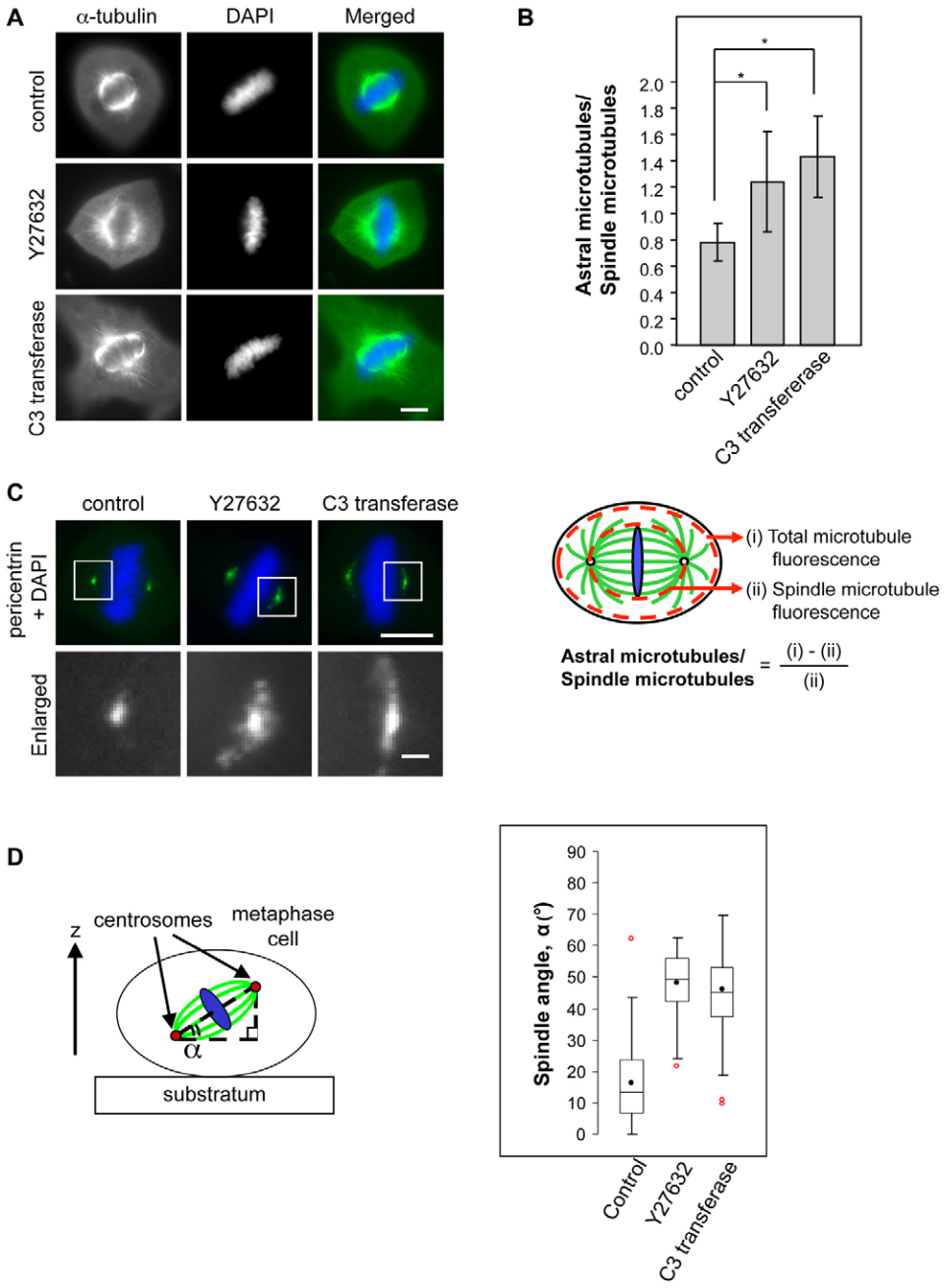

Fig. 1. The inhibition of Rho GTPases and ROCK affects astral microtubule arrangement, centrosome integrity and spindle orientation. (**A**) HeLa cells were treated with C3 transferase or Y27632 and immuno-stained with anti-α-tubulin antibody (green) and DAPI (blue). Scale bar, 10 µm. (**B**) The change in the numbers of astral microtubules was measured as a ratio of the astral microtubule fluorescence to the spindle fluorescence. The (i) total fluorescence of the tubulin stain and (ii) the fluorescence due to the spindle were measured. The fluorescence attributed to the astral microtubules was computed from the subtraction of the spindle fluorescence from the total fluorescence [(i)–(ii)]. Since the fluorescence of the spindle was found to be similar in the control and treated cells, we used the ratio of astral microtubule fluorescence/spindle fluorescence to compare the amount of astral microtubule changes in the control and treated cells. Twenty cells were analyzed per drug treatment. The mean and standard deviation (s.d.) of each experimental treatment are presented. Student's *t*-test was used to compute the significance of the difference. $*P<0.05$. (**C**) HeLa cells were treated as in A and immunostained with anti-pericentrin antibody (green) and DAPI (blue). The bottom panel represents an enlarged view of the boxed region. Scale bars, 10 µm. (**D**) HeLa cells were cultured on fibronectin-coated coverslips and treated as in A. Spindle angles with respect to the substratum were calculated as described in Materials and Methods. Box-and-whiskers diagram: box represents upper quartile, median and lower quartile; whiskers represent maximum and minimum, black dots represent mean, red circles represent outliers ($n\geq50$); experiment was performed in triplicate.

mutant of cofilin could cause changes to the actin cytoskeleton (supplementary material Fig. S1A, left column), no observable changes in microtubule arrangement were seen in interphase or metaphase cells transfected with cofilin wild-type, S3A or S3E mutant constructs (supplementary material Fig. S1A). Overexpression of slingshot, a phosphatase for cofilin, also could not induce excess astral microtubule formation (supplementary material Fig. S1B). These observations further support that cofilin is not involved in regulating the astral microtubules. Thus, RhoA and ROCK activities are required to ensure proper localization of LIMK2 to the mitotic spindle. Although LIMK2 kinase activity is crucial in the regulation of astral microtubules formation, cofilin is not involved in this process.

Rho–ROCK–LIMK2 pathway controls the astral microtubules dynamics by regulation of TPPP

As cofilin is not the LIMK2 substrate that participates in the regulation of astral microtubule, we searched for other possible proteins that can fulfil this role. TPPP is a microtubule polymerization-promoting protein, which is reported to be phosphorylated by LIMK1 (Acevedo et al., 2007). Therefore, we examined whether TPPP can also serve as a substrate for LIMK2 and mediate the regulation of astral microtubules. TPPP colocalized with the microtubule network at all stages of the cell cycle (supplementary material Fig. S2) – it also colocalized with LIMK2 at the mitotic spindle (Fig. 4A). Furthermore, TPPP showed physical interaction with both LIMK1 and LIMK2 in pull-down assays (Fig. 4B). In vitro kinase assays also showed

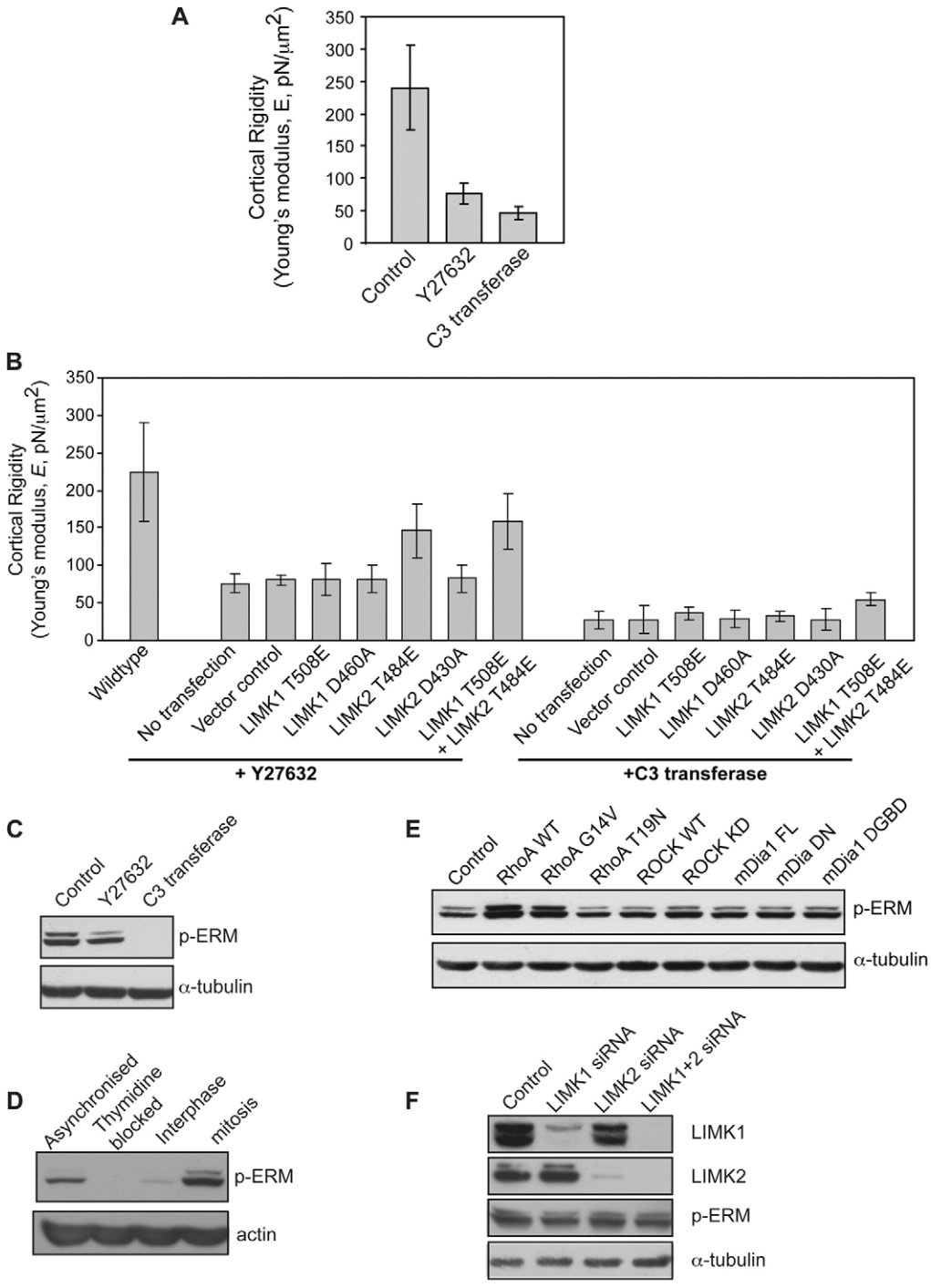

Fig. 2. LIMK cooperates with ERM proteins to regulate mitotic cortical rigidity. (**A**) HeLa cells were treated with Y27632 or C3 transferase. Mitotic cells were collected by 'shake-off' and subjected to the micropipette aspiration assay to measure cortical rigidity. Mean values of Young's Modulus, *E*, were plotted; error bars, s.d. ($n \geq 6$). The experiment was performed in triplicate. (**B**) Active LIMK2 can restore the loss in cortical rigidity induced by Y27632 treatment. HeLa cells were transfected with the vector, LIMK1- and LIMK2-active, and LIMK1- and LIMK2-inactive constructs. Transfected cells were treated with Y27632 or C3 transferase. Mitotic cells were collected by shake-off and subjected to the micropipette aspiration assay. The experiment was performed in triplicate; error bars, s.d. ($n \geq 6$). (**C**) Western blot analysis of mitotic shake-off cells treated with Y27632 and C3 transferase using antibodies against phosphorylated ERM and antibodies against α-tubulin (loading control). (**D**) Western blot analysis of cells in different phases of the cell cycle using antibodies against phosphorylated ERM and actin (loading control). (**E**) ERM phosphorylation during mitosis is not dependent on ROCK or mDia1. HeLa cells were transfected with various RhoA (wild type, dominant-active and dominant-negative mutants), ROCK [wild type (WT) and kinase domain (KD)] or mDia1 [full length (FL), dominant negative (DN) and active (*Δ*GBD)] constructs. Mitotic cells were collected by shake-off 24 hours post transfection, and cell lysates were subjected to western blot analysis using antibodies against phosphorylated ERM and antibodies against α-tubulin. (**F**) ERM phosphorylation is not affected by LIMK1 and LIMK2 knockdown. The experiments were conducted in a similar manner to E, but LIMK1 and LIMK2 siRNAs were transfected instead.

that TPPP could indeed be directly phosphorylated by both LIMK1 and LIMK2 (Fig. 4C).

Because TPPP colocalized and interacted with LIMK2 at the mitotic spindle, we examined whether Y27632 and C3 transferase treatment, or perturbation of LIMK could affect the spindle localization of TPPP. We found that Y27632 and C3 transferase treatment affected TPPP spindle-localization (Fig. 5A). The proportion of cells showing TPPP spindle localization after treatment with Y27632 and C3 transferase was reduced to 55% and 45%, respectively (Fig. 5B). In cells transfected with LIMK1 siRNA (for knockdown efficiency, see supplementary material Fig. S3A,C), TPPP was still able to localize to the mitotic spindle (Fig. 5A). By contrast, spindle localization of TPPP was greatly diminished in cells that were transfected with either LIMK2 siRNA alone or double-transfected with LIMK1 and LIMK2 siRNA, with only 37% and 24% of the cells exhibiting spindle localization, respectively (Fig. 5A,B). Active LIMK2 (T484E), but not active LIMK1 (T508E), restored TPPP spindle-localization upon treatment with Y27632 and C3 transferase (Fig. 5C). These results imply that TPPP localization to the mitotic spindle is largely dependent on the activity of Rho GTPases and ROCK, as well as the presence of LIMK2.

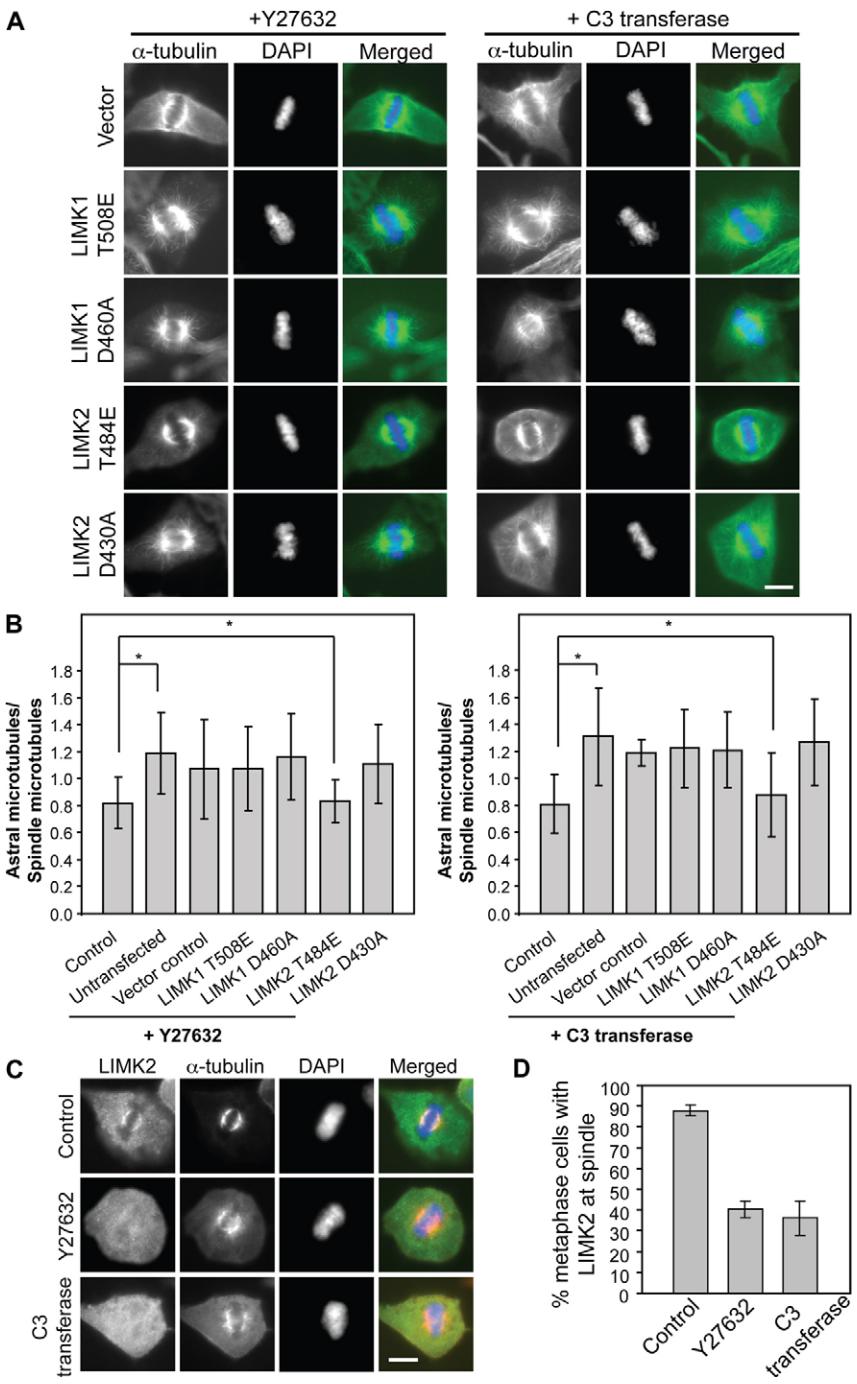

Fig. 3. LIMK2, but not LIMK1, regulates astral microtubule downstream of ROCK. (**A**) Rescue of the Y27632- and C3 transferase-induced astral microtubule phenotype by kinase-active LIMK2. HeLa cells were transfected with the mCherry (MC) vector control, MC–LIMK1–T508E, MC–LIMK1–D460A, MC–LIMK2–T484E or MC–LIMK2–D430A and subjected to Y27632 or C3 transferase treatment. Cells were immunostained with anti-α-tubulin (green) antibodies and DAPI (blue). Scale bar, 10 μm. (**B**) Quantification of astral microtubule fluorescence as in 1B. The Student's *t*-test was used. **P*<0.05. (**C**) Localization of LIMK2 to the mitotic spindle is dependent on RhoA and ROCK activity. HeLa cells were first treated with control solvent, Y27632 or C3 transferase and then with cytoskeleton buffer (10 mM MES pH 6.1, 138 mM KCl, 3 mM $MgCl_2$, 2 mM EGTA, 0.32 M sucrose) followed by methanol fixation. The cells were then immunostained with anti-LIMK2 (green) and anti-α-tubulin (red) antibodies, and DAPI (blue). Scale bar, 10 μm. (**D**) The average proportion of metaphase cells with LIMK2 spindle localization was scored. The experiment was performed in triplicate; error bars, s.d. ($n \geq 163$).

We then investigated whether TPPP regulates astral microtubules directly. Two siRNAs targeting different regions of the *TPPP* mRNA were designed (for knockdown efficiency, see supplementary material Fig. S3B,D). Silencing of *TPPP* did not result in any observable changes in the microtubule network or in the mitotic spindles in interphase and metaphase (supplementary material Fig. S4). However, the outcome was different when HeLa cells were treated with C3 transferase and Y27632. We found that in control cells transfected with luciferase siRNA, treatment with Y27632, C3 transferase or LIMK2 siRNA were able to cause excessive astral microtubule formation during metaphase (Fig. 5D, top panels). However, in cells transfected with TPPP siRNAs, there was a reduction in the number of astral microtubules in similarly treated cells (Fig. 5D,E). Thus, TPPP might only be required for the control of astral microtubule dynamics.

Rho–ROCK–LIMK2–TPPP pathway controls metaphase spindle-orientation

Next, we examined the spindle orientation, another phenotype that is affected by the inhibition of Rho GTPases and ROCK. Astral microtubules have long been thought to control the physical interaction between the mitotic spindle and the cell cortex and, hence, might influence the orientation and positioning

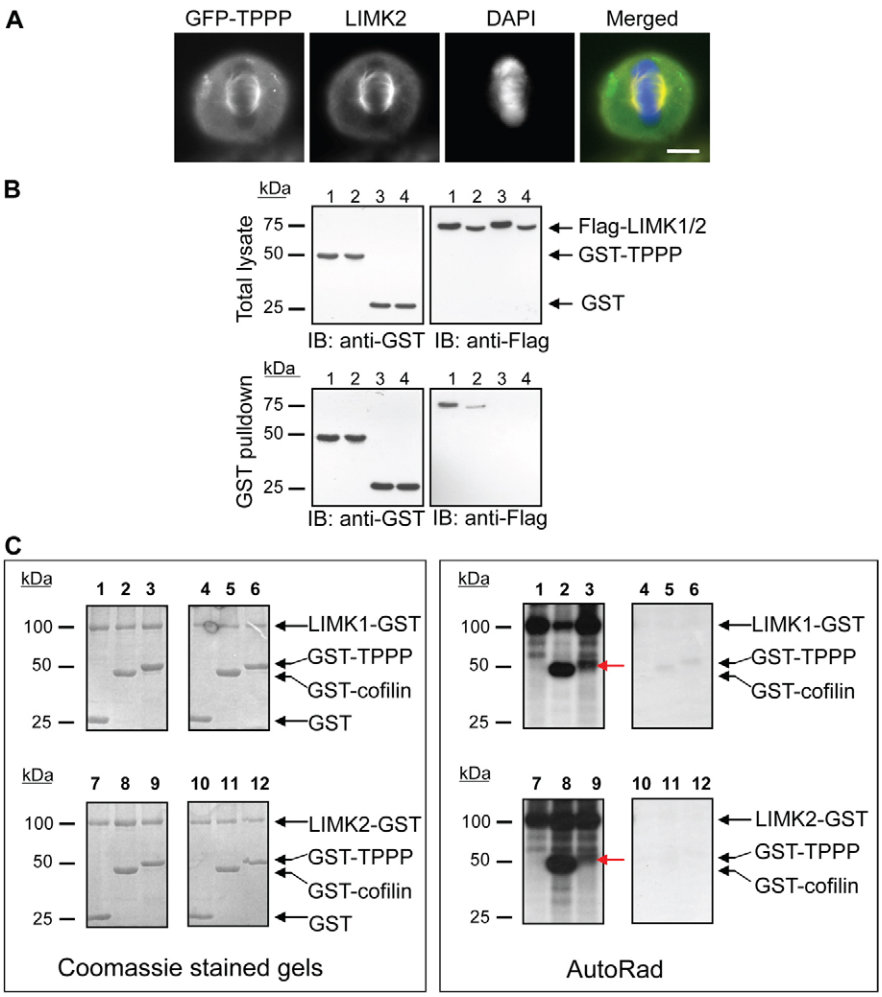

Fig. 4. TPPP is a downstream target of LIMK2. (**A**) TPPP colocalizes with LIMK2 at the mitotic spindle. HeLa cells were transfected with pXJΔ2–eGFP–TPPP (green), fixed with cytoskeleton buffer and immunostained with anti-LIMK2 antibodies (red) and DAPI (blue). Scale bar, 10 μm. (**B**) TPPP interacts with LIMK1 and LIMK2. HeLa cells were transfected with GST–TPPP or the GST control, and co-transfected with Flag–LIMK1 or Flag–LIMK2. Cell lysates were subjected to GST pull-down and western blot analysis by using antibodies against GST and Flag. Lane 1, GST–TPPP plus Flag–LIMK1; lane 2, GST–TPPP plus Flag–LIMK2; lane 3, GST plus Flag–LIMK1; lane 4, GST plus Flag–LIMK2. (**C**) In vitro kinase assay. C-terminal GST-tagged LIMK constructs were transfected into COS7 cells and pulled down for the kinase assay. Lane 1, LIMK1 (T508E) plus GST; lane 2, LIMK1 (T508E) plus cofilin; lane 3, LIMK1 (T508E) plus TPPP; lane 4, LIMK1 (D460A) plus GST; lane 5, LIMK1 (D460A) plus cofilin; lane 6, LIMK1 (D460A) plus TPPP; lane 7, LIMK2 (T484E) plus GST; lane 8, LIMK2 (T484E) plus cofilin; lane 9, LIMK2 (T484E) plus TPPP; lane 10, LIMK2 (D430A) plus GST; lane 11, LIMK2 (D430A) plus cofilin; lane 12, LIMK2 (D430A) plus TPPP. Red arrows indicate phosphorylated TPPP bands.

of the spindle in the mitotic cell (Hyman, 1989; Hyman and White, 1987). We found that in cells treated with Y27632 or C3 transferase, the angle of the spindle in relation to the substratum was increased (Fig. 1D), and only active LIMK2 (T484E) was able to rescue this mis-orientation to some degree (Fig. 6A,B). In cells treated with Y27632 and C3 transferase, knockdown of TPPP reduced the angle of spindle orientation (Fig. 6C). However, TPPP knockdown was only able to rescue spindle mis-orientation caused by LIMK2 siRNA, but not by LIMK1 siRNA or LIMK1 and LIMK2 double siRNA transfection (Fig. 6D). This suggests that RhoA, ROCK, LIMK1 and LIMK2 contribute to the control of the spindle angle during mitosis, but TPPP can only regulate spindle orientation downstream of LIMK2 but not LIMK1. It is possible that regulation of spindle orientation by LIMK1 is modulated by cofilin instead (Kaji et al., 2008). This further supports our hypothesis that TPPP functions downstream of LIMK2, regulating astral microtubule formation and, hence, the spindle orientation.

Loss of LIMK1 and LIMK2 signaling leads to defocused centrosomes

Because we observed defocusing of the centrosome in Y27632- and C3 transferase-treated cells at metaphase (Fig. 1C), we investigated whether the LIMK proteins are involved. We observed that silencing of LIMK1 and LIMK2 led to severe loss of centrosome integrity (Fig. 7A). In control cells transfected with siRNA targeting the luciferase gene, ~90% of the metaphase cells showed normal centrosomes and normal numbers of astral microtubules. However, silencing of LIMK1 led to 40% of the metaphase cells showing diffused (defocused) centrosomes and an increased number of astral microtubules (Fig. 7B). More than 50% of the LIMK1 knockdown cells exhibited multi-polar spindles. However, in LIMK2 knockdown cells, ~60% of the metaphase cells showed increased numbers of astral microtubules, but with normal centrosome morphology. Nevertheless, ~40% of the LIMK2-knockdown metaphase cells showed diffused centrosomes as well as increased astral microtubules (Fig. 7B). Silencing of both LIMK1 and LIMK2 resulted in the majority (80%) of the metaphase cells showing multi-polar spindles. The multi-polar spindles are unlikely to be due to cytokinesis failure, because cells treated with LIMK siRNAs do undergo cytokinesis (supplementary material Fig. S5). We also examined the cortical rigidity of LIMK1 and LIMK2 knockdown cells to determine whether cortical rigidity is affected. Indeed, silencing of LIMK1 and LIMK2 resulted in reduced cortical rigidity in metaphase cells (Fig. 7C). Although silencing of TPPP resulted in the loss of cortical rigidity (Fig. 7D), we did not observe many defocused centrosomes in TPPP-knockdown cells (Fig. 7E), suggesting that TPPP functions

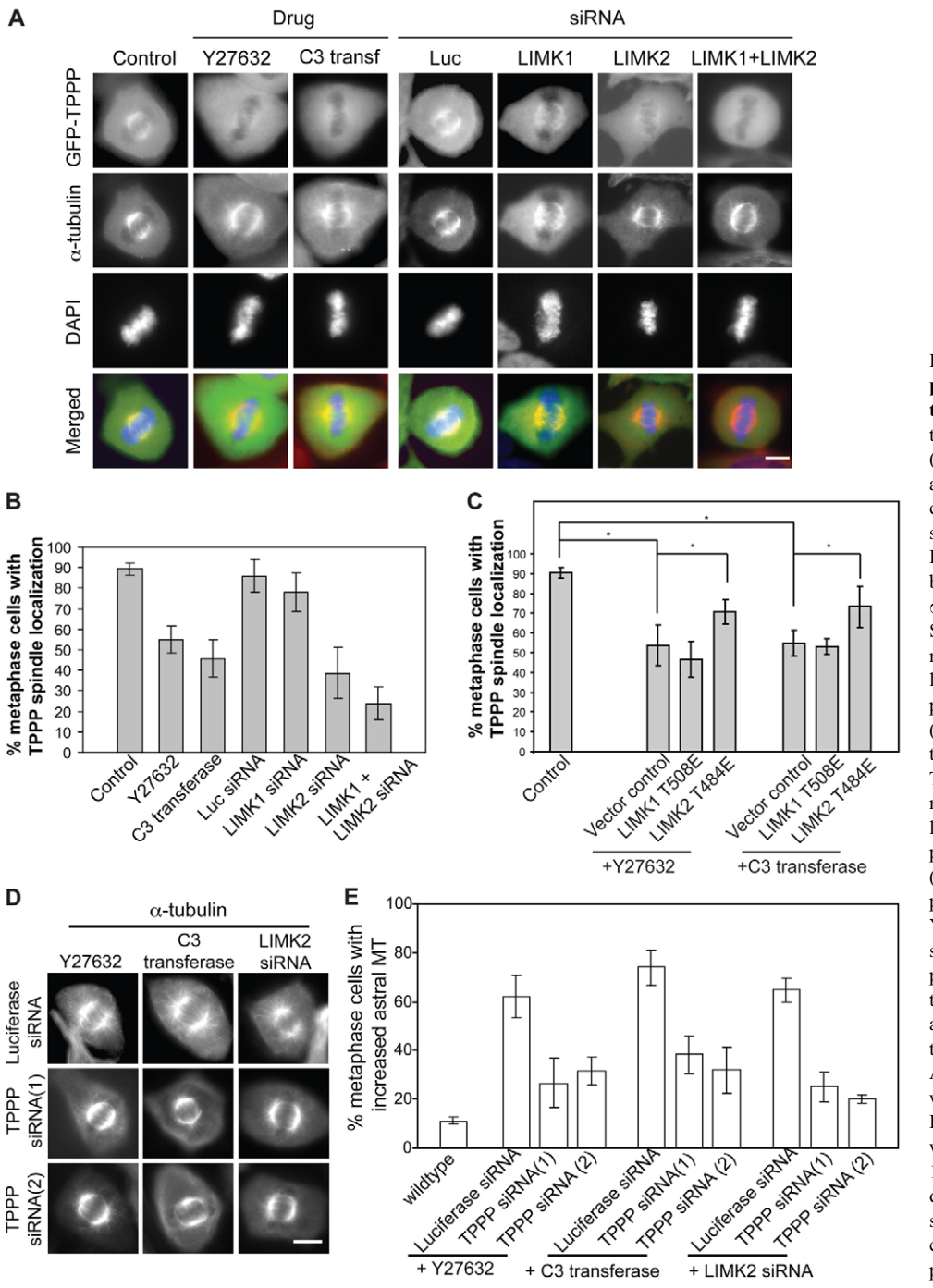

Fig. 5. The RhoA-ROCK-LIMK2 pathway controls localization of TPPP to the mitotic spindle. (**A**) HeLa cells were transfected with pXJΔ2–eGFP–TPPP (green) and treated with various drugs. In another set of experiments, HeLa cells were co-transfected with pXJΔ2–eGFP–TPPP and siRNAs targeting luciferase, LIMK1 and LIMK2. Cells were fixed with cytoskeleton buffer and methanol, and stained with anti-α-tubulin antibodies (red) and DAPI (blue). Scale bar, 10 μm. (**B**) The number of metaphase cells displaying TPPP spindle localization was scored, and mean percentages were plotted; error bars, s.d. ($n \geq 122$). The experiment was performed in triplicate. (**C**) Active LIMK2 can restore TPPP spindle localization. The number of metaphase cells displaying TPPP spindle localization was scored and mean percentages were plotted; error bars, s.d. ($n \geq 135$), $^*P < 0.05$. The experiment was performed in triplicate. (**D**) Rescue of the Y27632-, C3 transferase- and LIMK2 siRNA-induced astral microtubule phenotype by TPPP siRNA. HeLa cells were transfected with siRNA targeting luciferase and TPPP, and treated with Y27632 or C3 transferase, 48 hours post-transfection. Another set of HeLa cells was co-transfected with luciferase, or TPPP siRNA with LIMK2 siRNA. Cells were immunostained with antibodies against α-tubulin. Scale bar, 10 μm. (**E**) The number of metaphase cells displaying increased astral microtubules was scored and mean percentages were plotted; error bars, s.d. ($n \geq 44$). The experiment was performed in triplicate.

primarily in regulating the astral microtubules and, thus, cortical rigidity, but does not impact centrosome integrity. Our data suggest that disruption of cortical actin leads to diffused centrosomes and that LIMK1 and LIMK2 are responsible for the focusing of centrosomes. LIMK1 and LIMK2 are also implicated in the clustering of centrosomes to prevent multi-polar spindles.

Perturbation of actin cytoskeleton at early stages of mitosis resulted in aberrant astral microtubules

Thus far, we have used C3 transferase and Y27632 to disturb the actin structures. In order to test whether the perturbation of actin by other means could also elicit similar astral microtubule phenotypes, we used cytochalasin D (depolymerizes actin), jasplakinolide (stabilizes actin polymers), blebbistatin (inhibits myosin) and overexpression of α-actinin (increases bundling of actin filaments). We found that there were increased astral microtubules in all cases where actin cytoskeleton was perturbed (Fig. 8A,B). We also observed defocused centrosomes where the actin cytoskeleton was affected (Fig. 8C). As expected, the disruption (cytochalasin D treatment) or stabilization (jasplakinolide treatment and overexpression of α-actinin) of actin cytoskeleton resulted in decreased and increased cortical rigidity of the mitotic cells, respectively (Fig. 8D).

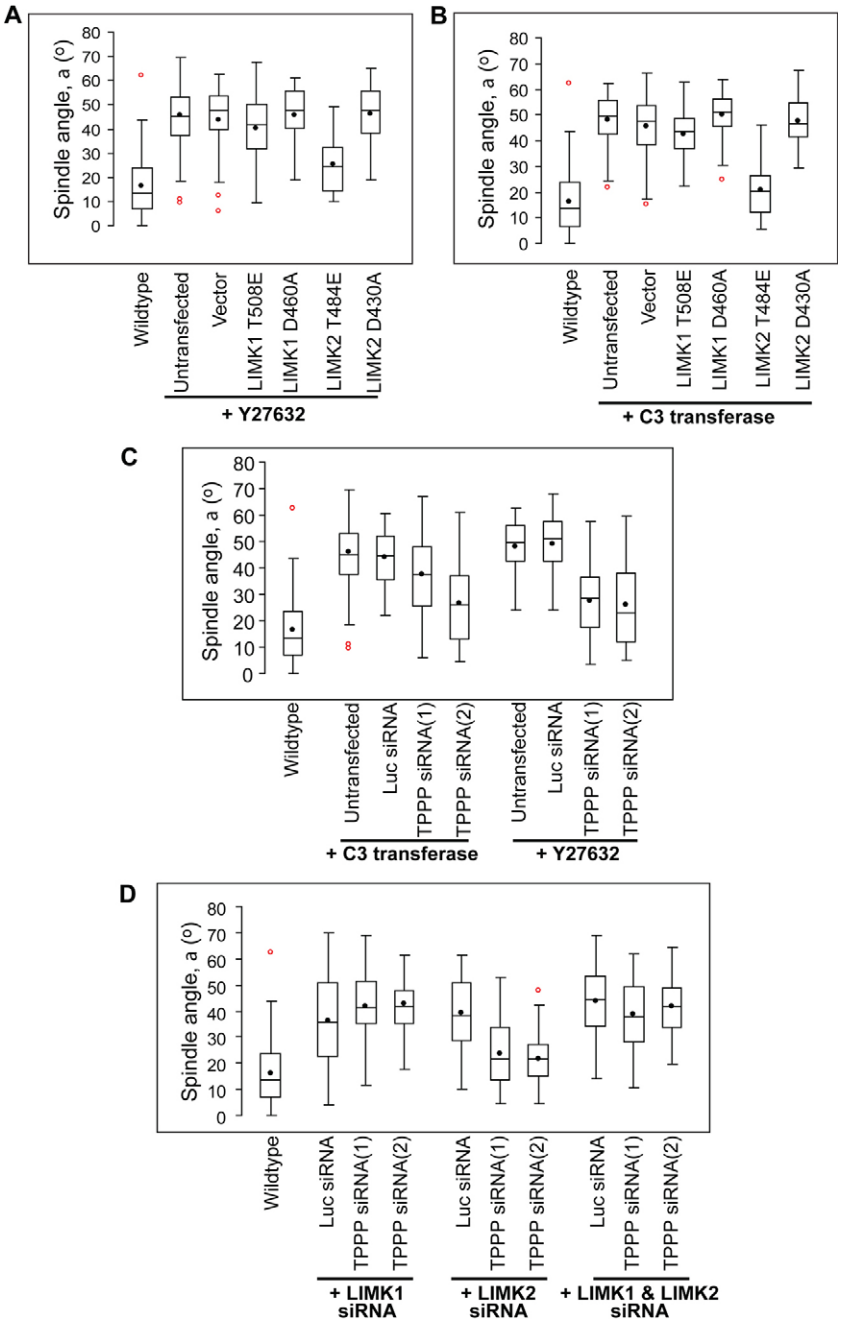

Fig. 6. Active LIMK2 as well as knockdown of TPPP can rescue spindle mis-orientation. (**A**) Rescue of Y27632-induced metaphase spindle misorientation by kinase-active LIMK2. The experiment was performed and the spindle angle measured as in Fig. 1D. (**B**) Rescue of C3 transferase-induced metaphase spindle misorientation by kinase-active LIMK2. The spindle angle measurement was performed as in A. (**C**) Rescue of Y27632- and C3 transferase-induced metaphase spindle misorientation by TPPP knockdown. HeLa cells were cultured on fibronectin-coated coverslips, transfected with luciferase siRNA, TPPP siRNA(1) or TPPP siRNA(2), and were treated with Y27632 or C3 transferase 48 hours post-transfection. The spindle angle measurement was performed as in A. (**D**) TPPP siRNAs were co-transfected with LIMK1 and LIMK2 siRNAs into HeLa cells grown on fibronectin-coated coverslips. The spindle angle was measured as in Fig. 1D. The experiments were performed in triplicate ($n \geq 50$).

Discussion

In this study we have explored the regulatory connections between the actin cytoskeleton and cell cycle progression, particularly during the early stages of mitosis. We find that perturbation of the actin structures prior to mitosis causes an increase in the number of astral microtubules, which in turn affects spindle orientation (Fig. 1). Moreover, we find that astral microtubule formation is dependent on the cortical rigidity because the disruption (cytochalasin D, blebbistatin, C3 transferase or Y27632 treatment) or the stabilization (jasplakinolide or α-actinin overexpression) of the actin network produced similar excessive astral microtubule phenotypes (Fig. 8). It appears that any perturbation in the cortical rigidity will result in changes in the numbers of astral microtubules. This is reminiscent of a report which suggests that when the levels of phosphatidylinositol-3,4,5-triphosphate [PtdIns(3,4,5)P3] are either too high or too low, the dynein–dynactin pulling force on the astral microtubule is dispersed and results in mis-orientation of the spindles (Toyoshima et al., 2007). Our observations suggest a strong correlation between the perturbation of cortical rigidity and the status of actin polymerization. We also find that the perturbation of the actin cytoskeleton substantially affects the astral microtubule numbers as well as centrosome integrity in the early stages of mitosis. The fact that the use of actin drugs such as cytochalasin D and jasplakinolide also causes the defocusing of the centrosomes (Fig. 8C) suggests that the actin cytoskeleton has an important role in the regulation of centrosomes. Although the finer details of the regulatory links between the actin cytoskeleton and mechanical properties of the

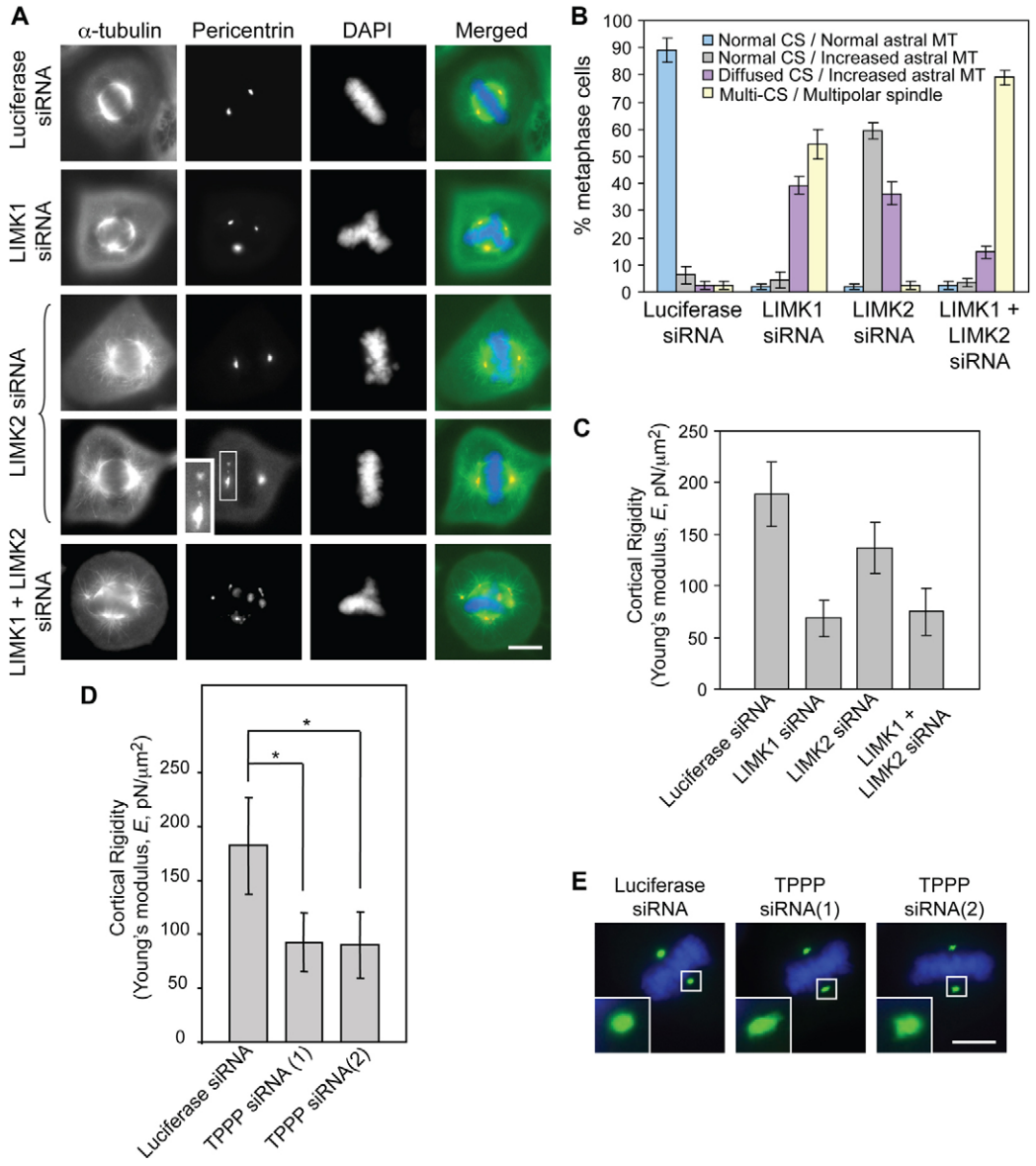

Fig. 7. Knockdown of LIMK1 and LIMK2 affects centrosome integrity and cortical rigidity during mitosis. (**A**) Increase in metaphase astral microtubules and diffused centrosomes after LIMK knockdown. HeLa cells were transfected with siRNA targeting luciferase, LIMK1, LIMK2 or LIMK1 plus LIMK2. After 48 hours, cells were immunostained with anti-α-tubulin (green) and anti-pericentrin (red) antibodies, and DAPI (blue). Scale bar, 10 μm. (**B**) The average percentage of metaphase cells in each phenotype category was scored; error bars represent the s.d. ($n=100$). The experiment was performed in triplicate. CS, centrosome; MT, microtubules. (**C**) Mitotic cortical rigidity decreases after LIMK knockdown. HeLa cells were transfected as in A. After 48 hours, mitotic cells were collected by shake-off and subjected to the micropipette aspiration assay for cortical rigidity. Mean values of Young's Modulus, E, were plotted; error bars, s.d. ($n=7$). The experiment was performed in triplicate. (**D**) TPPP knockdown affects the mitotic cortical rigidity. HeLa cells were transfected with luciferase and TPPP siRNAs. The mitotic cortical rigidity was measured as in C. Error bars, s.d. ($n=5$), $^*P<0.05$. (**E**) TPPP knockdown does not influence centrosome pericentrin staining. HeLa cells were transfected with luciferase and TPPP siRNAs. After 48 hours, the cells were fixed and immunostained with anti-pericentrin antibodies (green) and DAPI (blue). Scale bar, 10 μm.

cortex remain to be deciphered, we propose that perturbation to cortical rigidity can result in defects in astral microtubules.

In the current study, we have established the RhoA–ROCK–LIMK2–TPPP signaling pathway as the regulator of astral microtubules and spindle orientation during mitosis. Our observations suggest that only active LIMK2 is able to reverse the astral microtubule phenotype induced by C3 transferase or Y27632 treatment. Moreover, LIMK2 knockdown cells also showed an increase in astral microtubules (Fig. 5D, top right; Fig. 7). This suggests that LIMK2, but not LIMK1, acts downstream of RhoA and ROCK in the control of astral microtubule dynamics. Additional evidence comes from the observations that LIMK1 is localized to the centrosomes and LIMK2 to the mitotic spindles (Sumi et al., 2006). Knocking down LIMK2 also increases the number of abnormal spindles in cells treated with microtubule-destabilizing drugs (Po'uha et al., 2010). Interestingly, it has also been reported that ROCK phosphorylates LIMK2 downstream of RhoA activation (Sumi

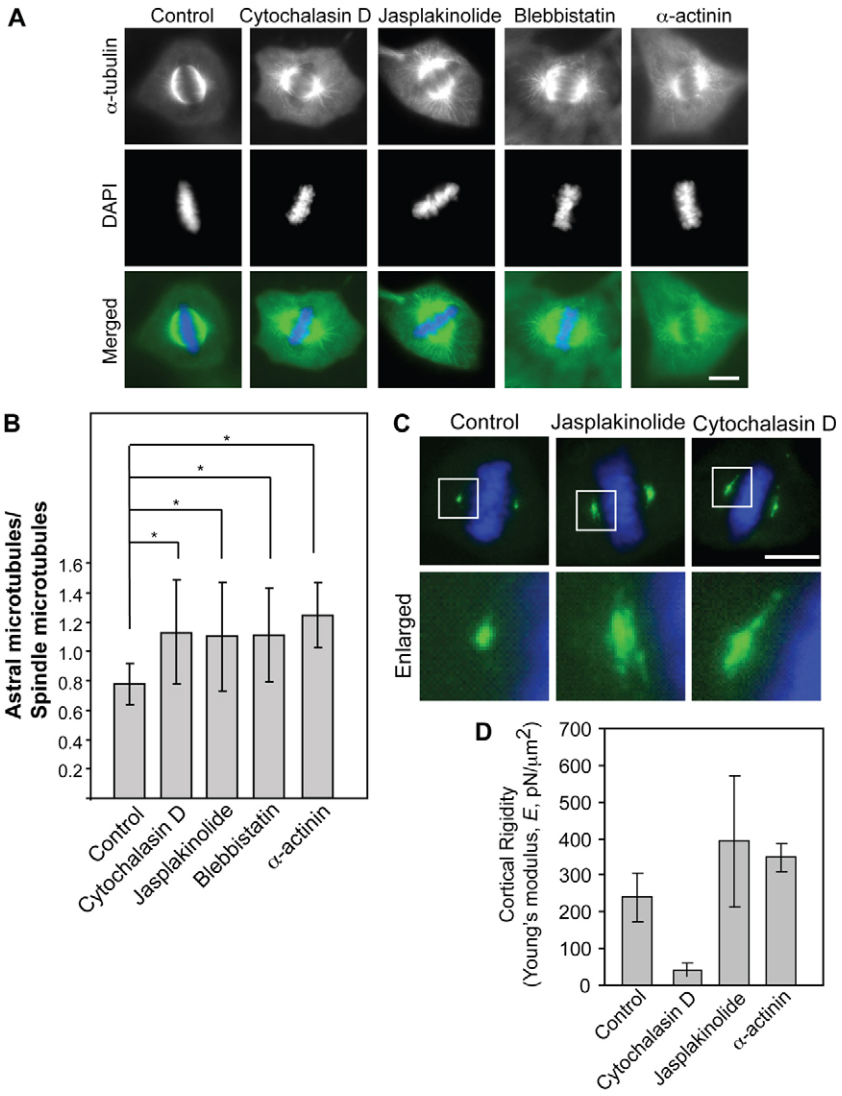

Fig. 8. The treatment of HeLa cells with actin drugs affects cortical astral microtubule arrangement, centrosome integrity and cortical rigidity. (**A**) HeLa cells were treated with cytochalasin D, jasplakinolide and blebbistatin for 3 hours, and in a separate experiment were transfected with α-actinin cDNA for 24 hours. The cells were fixed and immunostained with anti-α-tubulin (green) antibodies and DAPI (blue). Scale bar, 10 μm. (**B**) The increase in astral microtubules was quantified as in Fig. 1B. *$P<0.05$. (**C**) HeLa cells were treated separately with jasplakinolide and cytochalasin D for 3 hours. The cells were fixed and immunostained with anti-pericentrin (green) antibodies and DAPI (blue). The lower panels show an enlarged view of the boxed areas. Scale bar, 10 μm. (**D**) Mitotic cells were collected by shake-off and subjected to the micropipette aspiration assay. The experiment was performed in triplicate; error bars, s.d. ($n\geq6$).

et al., 2001), but not LIMK1, which is phosphorylated by the PAK kinases (Edwards et al., 1999).

It has been reported that phosphorylation of TPPP inhibits its tubulin polymerizing activity (Acevedo et al., 2007; Hlavanda et al., 2007). Therefore, our data suggest that under normal circumstances, LIMK2 present at the mitotic spindle phosphorylates TPPP and prevents excessive tubulin polymerization, thus, controlling the number of astral microtubule filaments. In the event of RhoA or ROCK inhibition, activity of LIMK2 at the spindle is decreased; consequently, the levels of TPPP phosphorylation are also reduced. This renders TPPP active and results in enhanced microtubule polymerization, leading to increased astral microtubules numbers.

Aberrant astral microtubule organization can further affect the positioning and orientation of the mitotic spindle. In cells growing in the culture dish, the orientation of the spindle might not be as crucial. However, spindle orientation is particularly important for polarized cell types and for asymmetric cell divisions where the division planes are crucial for the development of the organism as a whole (Gönczy, 2008). Our results suggest that the RhoA–ROCK–LIMK2–TPPP pathway is required in the positioning of the spindles. We proposed that LIMK2 acts through TPPP to functionally connect actin cytoskeleton signaling and cell cycle activities controlled by the microtubules.

This study also reveals a possible connection between the cortical actin network and centrosome integrity, in that perturbation of the actin cytoskeletal network results in the defocusing of centrosomes. LIMK1 and LIMK2 are important in the regulation of centrosome focusing because loss of both LIMK1 and LIMK2 resulted in the majority of metaphase cells showing multi-polar spindles. Over-duplication of the centrosomes is one of the causes of chromosome instability in cancer cells (Fukasawa, 2007). Chromosome segregation mediated by multi-polar spindles can lead to aneuploidy. Our observations suggest that, apart from maintaining the focusing of centrosomes, LIMK1 and LIMK2 are also involved in the regulation of centrosome duplication and/or clustering. Whether centrosome duplication or clustering is directly regulated by LIMKs or actin cytoskeleton cues is not clear because silencing LIMK1 and LIMK2 also leads to lower cortical rigidity. It is conceivable that LIMK is one of the actin cytoskeletal effectors that control the number of astral microtubules and clustering of centrosomes. Taken together, our results show the importance of LIMK1 and LIMK2 in the regulation of centrosome integrity and

clustering, which is crucial for orderly cell division to avoid aneuploidy.

Materials and Methods

Cell culture and drug treatment

HeLa cells were maintained in minimum essential medium (MES) (Sigma) supplemented with 10% fetal bovine serum in a humidified incubator at 37℃ in 5% CO_2. Unless otherwise stated, cells were treated with 30 μM Y27632 (Calbiochem) and 2.0 μg/ml cell-permeable C3 transferase (Cytoskeleton Inc., Denver, USA), for 3 hours before the assays. Other drug treatments include 100 μM blebbistatin (Sigma), 0.5 μg/ml cytochalasin D (Sigma), and 50 μM jasplakinolide (Invitrogen). The drugs and chemicals were dissolved in the appropriate solvent, as suggested by the manufacturers.

Plasmids and siRNA

LIMK mutants were generated using a QuikChange Site-Directed Mutagenesis Kit (Stratagene) according to the manufacturer's protocol. All constructs were cloned into a pXJ40-based vector. Stealth siRNAs were from Invitrogen. The sequences of siRNA (antisense) used were as follows: LIMK1, 5′-CAGUGUUCCAGCUUCACAAAGGAUG-3′; LIMK2, 5′-AAUAGCUGUUGGAACAACGAAGGGA-3′; TPPP(1), 5′-CAAGACUUCCCUUUGAUCUUGCUGA-3′; TPPP(2), 5′-UUGUCUUUGAAUCGCUUCUUGGCGA-3′; luciferase, 5′-UCGAAGUAUUCCGCGUACGUGAUGU-3′.

Antibodies and microscopy

Cytoskeleton buffer (10 mM MES pH 6.1, 138 mM KCl, 3 mM $MgCl_2$, 2 mM EGTA, 0.32 M sucrose) was used before permeabilization of the cells for cell staining. Antibodies used include mouse monoclonal anti-α-tubulin (Sigma-Aldrich), anti-hemagglutinin (HA) (Zymed-Invitrogen) and anti-Flag (Sigma-Aldrich) antibodies; and rabbit polyclonal anti-pericentrin (Abcam), anti-LIMK2 (Santa Cruz Biotechnology), anti-phosphorylated ERM (Cell Signaling Technology, Beverly, MA, USA) and anti-GST (Bethyl Laboratories, Montgomery, TX, USA) antibodies. Images were acquired with an Axio Observer microscope (Carl Zeiss, Germany, Tucson, AZ, USA) coupled to a Coolsnap HQ^2 camera (Photometrics) and analysed using MetaMorph software (Molecular Devices, Sunnyvale, CA, USA).

Astral microtubule measurement

HeLa cells were treated with Y27632, C3 transferase or other actin drugs 3 hours before fixation for immunostaining using anti-α-tubulin antibodies. The total fluorescence of the tubulin stain (i) and the fluorescence due to the spindle (ii) were measured (Fig. 1B). The fluorescence attributed to the astral microtubules was computed by subtracting the spindle fluorescence from the total fluorescence [(i) – (ii)]. As the fluorescence of the spindle was similar in the control and treated cells, we used the ratio of astral microtubule fluorescence to spindle fluorescence to compare the amount of astral microtubule changes in the control and treated cells.

Centrosome quantification

For the determination of centrosome diffusion and/or defocusing, asynchronized HeLa cells were fixed and stained using anti-pericentrin antibodies. Random metaphase cells were selected and imaged at fixed microscope camera exposure settings. The total fluorescence intensity was measured in an area of 50 by 50 pixel, with the individual centrosome centered within this selected area. The intensities were corrected for signal to noise ratio.

Micropipette aspiration assay

Mitotic cells were collected by 'shake-off' and re-suspended in smaller volumes. Cells were suspended in a covered glass chamber and subjected to aspiration using a glass micropipette of diameter ranging from 7.8 to 13.1 μm, and coated with 1% bovine serum albumin (BSA). Suction pressure was controlled using a precision pump (Cole-Parmer) with a flow rate between 20 to 60 ml/hr. Images were acquired every 9 seconds using 100× objective bright field microscope (Leica, Germany). Cortical deformation was measured using MetaMorph software, and Young's Modulus, E, was calculated as described by Robert Hochmuth (Hochmuth, 2000).

In vitro kinase assay

GST C-terminal-tagged kinase constructs were transfected into COS7 cells. The GST fusion proteins were pulled down and used for in vitro kinase assays. The substrates were produced in *Escherichia coli*. About 5 μg of substrates were used per kinase reaction. The pulled down kinases were washed with kinase buffer and then incubated with the substrates in 30 μl of the same buffer containing 500 μM ATP and 10 μCi [γ-^{32}P]ATP. The reaction mixtures were incubated at 30℃ for 30 minutes and the reactions were stopped by the addition of the SDS sample buffer. The reaction mixtures were then separated by SDS-PAGE. Protein gels were stained with Coomassie Blue and exposed to X-ray films.

Spindle-orientation assay

Cells were cultured on fibronectin-coated (Sigma-Aldrich) coverglass with a coating density of 3 μg/cm^2. After various treatments, cells were fixed and stained with anti-pericentrin antibodies and DAPI, and imaged. Z-stack images of metaphase cells were captured at 1 μm apart and the spindle angle relative to the substratum was calculated using inverse trigonometry functions.

Acknowledgements

We thank Zhang Rou, National University of Singapore for assistance in some of the micropipette assays.

Funding

This study was supported by the Academic Research Fund [grant number 10/1/22/19/659 to C.G.K.]; and Biomedical Research Council [grant number T206B3206-RS to C.G.K.].

Supplementary material available online at
http://jcs.biologists.org/lookup/suppl/doi:10.1242/jcs.096818/-/DC1

References

Acevedo, K., Li, R., Soo, P., Suryadinata, R., Sarcevic, B., Valova, V. A., Graham, M. E., Robinson, P. J. and Bernard, O. (2007). The phosphorylation of p25/TPPP by LIM kinase 1 inhibits its ability to assemble microtubules. *Exp. Cell Res.* **313**, 4091-4106.

Arber, S., Barbayannis, F. A., Hanser, H., Schneider, C., Stanyon, C. A., Bernard, O. and Caroni, P. (1998). Regulation of actin dynamics through phosphorylation of cofilin by LIM-kinase. *Nature* **393**, 805-809.

Bement, W. M., Benink, H. A. and von Dassow, G. (2005). A microtubule-dependent zone of active RhoA during cleavage plane specification. *J. Cell Biol.* **170**, 91-101.

Burridge, K. and Wennerberg, K. (2004). Rho and Rac take center stage. *Cell* **116**, 167-179.

Carreno, S., Kouranti, I., Glusman, E. S., Fuller, M. T., Echard, A. and Payre, F. (2008). Moesin and its activating kinase Slik are required for cortical stability and microtubule organization in mitotic cells. *J. Cell Biol.* **180**, 739-746.

Edwards, D. C., Sanders, L. C., Bokoch, G. M. and Gill, G. N. (1999). Activation of LIM-kinase by Pak1 couples Rac/Cdc42 GTPase signalling to actin cytoskeletal dynamics. *Nat. Cell Biol.* **1**, 253-259.

Etienne-Manneville, S. and Hall, A. (2002). Rho GTPases in cell biology. *Nature* **420**, 629-635.

Fukasawa, K. (2007). Oncogenes and tumour suppressors take on centrosomes. *Nat. Rev. Cancer* **7**, 911-924.

Gachet, Y., Tournier, S., Millar, J. B. and Hyams, J. S. (2001). A MAP kinase-dependent actin checkpoint ensures proper spindle orientation in fission yeast. *Nature* **412**, 352-355.

Gönczy, P. (2008). Mechanisms of asymmetric cell division: flies and worms pave the way. *Nat. Rev. Mol. Cell Biol.* **9**, 355-366.

Heng, Y. W. and Koh, C. G. (2010). Actin cytoskeleton dynamics and the cell division cycle. *Int. J. Biochem. Cell Biol.* **42**, 1622-1633.

Hlavanda, E., Klement, E., Kókai, E., Kovács, J., Vincze, O., Tökési, N., Orosz, F., Medzihradszky, K. F., Dombrádi, V. and Ovádi, J. (2007). Phosphorylation blocks the activity of tubulin polymerization-promoting protein (TPPP): identification of sites targeted by different kinases. *J. Biol. Chem.* **282**, 29531-29539.

Hochmuth, R. M. (2000). Micropipette aspiration of living cells. *J. Biomech.* **33**, 15-22.

Hyman, A. A. (1989). Centrosome movement in the early divisions of Caenorhabditis elegans: a cortical site determining centrosome position. *J. Cell Biol.* **109**, 1185-1193.

Hyman, A. A. and White, J. G. (1987). Determination of cell division axes in the early embryogenesis of Caenorhabditis elegans. *J. Cell Biol.* **105**, 2123-2135.

Kaji, N., Muramoto, A. and Mizuno, K. (2008). LIM kinase-mediated cofilin phosphorylation during mitosis is required for precise spindle positioning. *J. Biol. Chem.* **283**, 4983-4992.

Koh, C. G. (2006). Rho GTPases and their regulators in neuronal functions and development. *Neurosignals* **15**, 228-237.

Kunda, P. and Baum, B. (2009). The actin cytoskeleton in spindle assembly and positioning. *Trends Cell Biol.* **19**, 174-179.

Kunda, P., Pelling, A. E., Liu, T. and Baum, B. (2008). Moesin controls cortical rigidity, cell rounding, and spindle morphogenesis during mitosis. *Curr. Biol.* **18**, 91-101.

Kwon, M., Godinho, S. A., Chandhok, N. S., Ganem, N. J., Azioune, A., Thery, M. and Pellman, D. (2008). Mechanisms to suppress multipolar divisions in cancer cells with extra centrosomes. *Genes Dev.* **22**, 2189-2203.

Lee, K. and Song, K. (2007). Actin dysfunction activates ERK1/2 and delays entry into mitosis in mammalian cells. *Cell Cycle* **6**, 1486-1495.

Maekawa, M., Ishizaki, T., Boku, S., Watanabe, N., Fujita, A., Iwamatsu, A., Obinata, T., Ohashi, K., Mizuno, K. and Narumiya, S. (1999). Signaling from Rho to the actin cytoskeleton through protein kinases ROCK and LIM-kinase. *Science* **285**, 895-898.

Narumiya, S., Morii, N., Sekine, A. and Kozaki, S. (1990). ADP-ribosylation of the rho/rac gene products by botulinum ADP-ribosyltransferase: identity of the enzyme and effects on protein and cell functions. *J. Physiol. (Paris)* **84**, 267-272.

Ohashi, K., Nagata, K., Maekawa, M., Ishizaki, T., Narumiya, S. and Mizuno, K. (2000). Rho-associated kinase ROCK activates LIM-kinase 1 by phosphorylation at threonine 508 within the activation loop. *J. Biol. Chem.* **275**, 3577-3582.

Olson, M. F., Ashworth, A. and Hall, A. (1995). An essential role for Rho, Rac, and Cdc42 GTPases in cell cycle progression through G1. *Science* **269**, 1270-1272.

Po'uha, S. T., Shum, M. S., Goebel, A., Bernard, O. and Kavallaris, M. (2010). LIM-kinase 2, a regulator of actin dynamics, is involved in mitotic spindle integrity and sensitivity to microtubule-destabilizing drugs. *Oncogene* **29**, 597-607.

Rosenblatt, J., Cramer, L. P., Baum, B. and McGee, K. M. (2004). Myosin II-dependent cortical movement is required for centrosome separation and positioning during mitotic spindle assembly. *Cell* **117**, 361-372.

Sumi, T., Matsumoto, K., Takai, Y. and Nakamura, T. (1999). Cofilin phosphorylation and actin cytoskeletal dynamics regulated by rho- and Cdc42-activated LIM-kinase 2. *J. Cell Biol.* **147**, 1519-1532.

Sumi, T., Matsumoto, K. and Nakamura, T. (2001). Specific activation of LIM kinase 2 via phosphorylation of threonine 505 by ROCK, a Rho-dependent protein kinase. *J. Biol. Chem.* **276**, 670-676.

Sumi, T., Hashigasako, A., Matsumoto, K. and Nakamura, T. (2006). Different activity regulation and subcellular localization of LIMK1 and LIMK2 during cell cycle transition. *Exp. Cell Res.* **312**, 1021-1030.

Takenawa, T. and Miki, H. (2001). WASP and WAVE family proteins: key molecules for rapid rearrangement of cortical actin filaments and cell movement. *J. Cell Sci.* **114**, 1801-1809.

Théry, M., Racine, V., Pépin, A., Piel, M., Chen, Y., Sibarita, J. B. and Bornens, M. (2005). The extracellular matrix guides the orientation of the cell division axis. *Nat. Cell Biol.* **7**, 947-953.

Toyoshima, F. and Nishida, E. (2007). Integrin-mediated adhesion orients the spindle parallel to the substratum in an EB1- and myosin X-dependent manner. *EMBO J.* **26**, 1487-1498.

Toyoshima, F., Matsumura, S., Morimoto, H., Mitsushima, M. and Nishida, E. (2007). PtdIns(3,4,5)P3 regulates spindle orientation in adherent cells. *Dev. Cell* **13**, 796-811.

Uehata, M., Ishizaki, T., Satoh, H., Ono, T., Kawahara, T., Morishita, T., Tamakawa, H., Yamagami, K., Inui, J., Maekawa, M. et al. (1997). Calcium sensitization of smooth muscle mediated by a Rho-associated protein kinase in hypertension. *Nature* **389**, 990-994.

Yamamoto, M., Marui, N., Sakai, T., Morii, N., Kozaki, S., Ikai, K., Imamura, S. and Narumiya, S. (1993). ADP-ribosylation of the rhoA gene product by botulinum C3 exoenzyme causes Swiss 3T3 cells to accumulate in the G1 phase of the cell cycle. *Oncogene* **8**, 1449-1455.

Yang, N., Higuchi, O., Ohashi, K., Nagata, K., Wada, A., Kangawa, K., Nishida, E. and Mizuno, K. (1998). Cofilin phosphorylation by LIM-kinase 1 and its role in Rac-mediated actin reorganization. *Nature* **393**, 809-812.